JCIM JOURNAL OF CHEMICAL INFORMATION AND MODELING

pubs.acs.org/jcim Article

De Novo Structure-Based Drug Design Using Deep Learning

Sowmya Ramaswamy Krishnan,[#] Navneet Bung,[#] Sarveswara Rao Vangala, Rajgopal Srinivasan, Gopalakrishnan Bulusu, and Arijit Roy*

Cite This: *J. Chem. Inf. Model.* 2022, 62, 5100−5109 Read Online

ACCESS | Metrics & More | Article Recommendations | Supporting Information

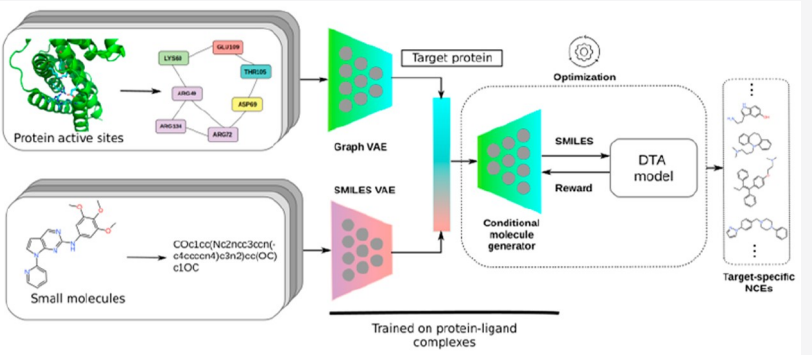

ABSTRACT: In recent years, deep learning-based methods have emerged as promising tools for *de novo* drug design. Most of these methods are ligand-based, where an initial target-specific ligand data set is necessary to design potent molecules with optimized properties. Although there have been attempts to develop alternative ways to design target-specific ligand data sets, availability of such data sets remains a challenge while designing molecules against novel target proteins. In this work, we propose a deep learning-based method, where the knowledge of the active site structure of the target protein is sufficient to design new molecules. First, a graph attention model was used to learn the structure and features of the amino acids in the active site of proteins that are experimentally known to form protein−ligand complexes. Next, the learned active site features were used along with a pretrained generative model for conditional generation of new molecules. A bioactivity prediction model was then used in a reinforcement learning framework to optimize the conditional generative model. We validated our method against two well-studied proteins, Janus kinase 2 (JAK2) and dopamine receptor D2 (DRD2), where we produce molecules similar to the known inhibitors. The graph attention model could identify the probable key active site residues, which influenced the conditional molecule generator to design new molecules with pharmacophoric features similar to the known inhibitors.

INTRODUCTION

One of the primary efforts to cure diseases involves the identification of therapeutic molecules that can modulate the activity of proteins responsible for diseases. Various computational methods have been developed to improve the success rate of the drug design process. Recent advancements and applications of deep learning-based methods in the field of drug design[1−3] have led to a surge of interest and hope toward accelerating the drug design process. Indeed, there are several advantages of these methods. One of the major advantages includes the exploration of the potentially unexplored chemical space,[4] which is estimated to be 10^{60}. It has also been shown that deep learning methods not only explore the vast chemical space but also can design new molecules with on-the-fly physicochemical property optimization toward a specific target protein.[5−13] The time from early stage drug design and optimization to experimental validation, has been drastically reduced with the help of deep learning methods.[14,15]

The drug design approaches against a target protein of interest can be broadly classified into ligand-based drug design and structure-based drug design. A majority of the deep learning-based drug design studies are ligand-based, which use the existing knowledge of target-specific small molecules to design a set of more potent target-specific molecules with optimized properties through transfer learning and/or reinforcement learning.[6,9,14] While ligand-based drug design methods have provided reliable results for several popular drug targets, their dependence on a data set of existing target-specific ligands restricts their utility against novel target proteins and proteins with limited known ligand data.

Special Issue: Computational Chemistry in Asia

Received: November 1, 2021
Published: November 18, 2021

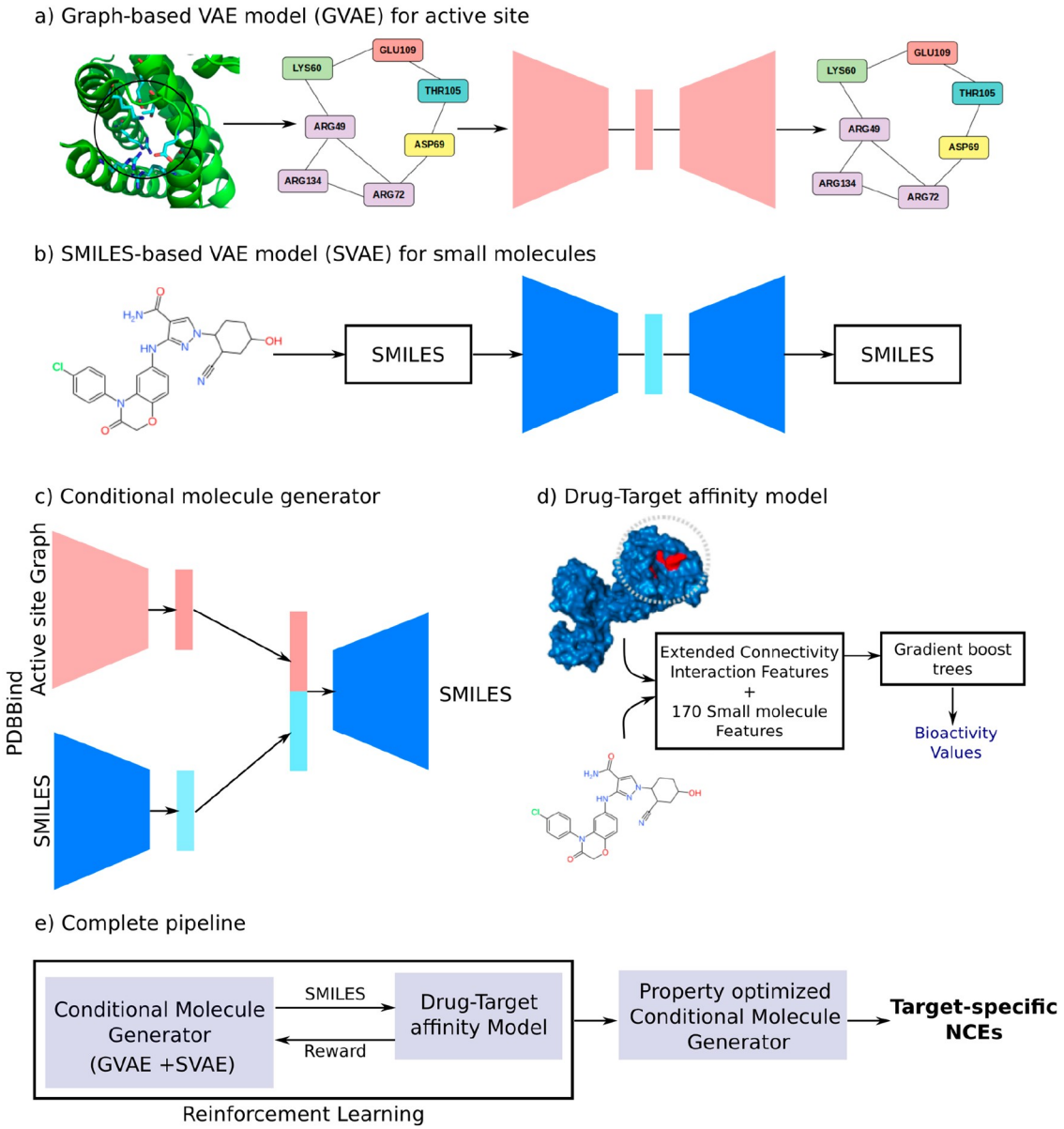

Figure 1. Structure-based drug design pipeline. The components of the pipeline are as follows: (a) pretraining the GAT-VAE model to learn the active site graph; (b) Pretraining the SMILES-VAE model to learn the grammar of small molecules; (c) combining the GAT-VAE and SMILES-VAE model to form the conditional molecule generator; (d) pretraining the drug-target affinity (DTA) prediction model to predict bioactivity of generated small molecules; (e) fine-tuning the conditional molecule generator (agent) using the DTA model (critic) in a reinforcement learning framework.

In contrast, the structure-based drug design approach relies only on the structural features of the target protein to generate small molecules with complementary features which facilitate better binding. Traditionally structure-based drug design utilizes fragment growing and/or fragment linking methods.[16] A few recent studies have also applied deep learning techniques to utilize the protein structure information for *de novo* design of novel small molecules.[3,8,17,18] Such studies can be broadly classified into two categories: namely, unsupervised and semisupervised methods.

Among the structure-based drug design approaches using deep learning, one study[17] utilized graph representations of both the binding site and ligand, and another study[3] utilized a voxelized representation of the protein binding site to predict Simplified Molecular Input Line Entry System (SMILES) corresponding to the predicted complementary ligand shapes. Both of the above studies can be categorized as unsupervised binding site-based molecule generation approaches.

On the other hand, recent works[8,18] have utilized the entire protein sequence as input to the generative model. Grechishnikova et al.[18] has used an unsupervised approach where, the protein sequence was encoded into a latent representation by the encoder, which was used by a SMILES decoder to generate target-specific small molecules. Another study[8] reported the application of reinforcement learning-based training to the generation of target-specific molecules using a complete protein sequence. These studies can be categorized as unsupervised and semisupervised protein sequence-based molecule generation approaches, respectively.

In this study, we propose a semisupervised multimodal deep learning model utilizing a graph representation of the protein binding sites and SMILES representation of the ligand to

https://doi.org/10.1021/acs.jcim.1c01319
J. Chem. Inf. Model. 2022, 62, 5100−5109

design novel small molecules for any target protein of known structure. The graph and SMILES models are combined to form a target-specific molecule generator, which is subject to a short retraining phase prior to further optimization. Next, a multimodal drug-target affinity (DTA) prediction model is used to formulate a reward function for target-specific bioactivity maximization, which is utilized as the objective to optimize the molecule generation process in a reinforcement learning framework. To the best of our knowledge, this is the first method to utilize the binding site representation of a protein in a semisupervised setting to steer the molecule generation process. Using this method, molecules were designed against two well studied protein targets, JAK2 and DRD2, and compared against known inhibitors of these proteins. The method could produce both similar and identical molecules compared to the existing inhibitors, while also retaining diversity. The generated molecules also preserved features of the existing inhibitors although the model had information about only the active site of the target proteins. Finally, based on the graph attention model, a set of key active site residues were identified which could be responsible for favorable features of the generated new chemical entities.

MATERIALS AND METHODS

To design novel small molecules by utilizing the active site information of the target protein, first the active site is represented as a graph to learn the structure and type of interactions from amino acids lining the active sites. A multihead graph attention (GAT) neural network is used to embed the active site graphs.[19] SMILES[20] is used to represent the small molecules, whose grammar is captured by a recurrent neural network (RNN).[21] Next, variational autoencoders (VAE) are used to learn both the active site and small molecule embeddings.[11] The active site graph embedding was utilized to condition the generative process. A reinforcement learning (RL) framework is used with a conditional molecule generator (a combination of the pretrained graph and SMILES-VAEs) as the agent, and a pretrained drug-target affinity (DTA) prediction model as the critic. The following sections describe the method in detail.

Representing the Active Site of a Target Protein as a Graph. The active site of a target protein is composed of key amino acid residues which interact with a small molecule (ligand). Since we assume that the small molecules capable of binding to the protein are unknown *a priori*, the representation of the active site is ligand-agnostic. At this stage, the aim of the model is to learn the structure and the type of interactions between the different amino acid residues in the active site. The active site is represented as a graph where nodes represent amino acids, and edges represent the interaction between two amino acids within a predefined distance cutoff from each other[22,23] (Figure S1b). In this way, the constructed active site graph resembles an atom pair contact network.[24] The nodes of the graph are featurized by classifying the amino acids into one of seven classes based on volume and dipole moment,[25] along with their ability to act as hydrogen bond donor and hydrogen bond acceptor, leading to a total of nine node features. The unweighted adjacency matrix and the one-hot encoded node feature vector of the active site graph are provided as input to the GAT-VAE model.

Pretraining the GAT-VAE Model to Encode the Active Site Graph. *Data.* The data set of active sites was collated from the PDBbind[26] and scPDB[27] databases. PDBbind database (v2019) is composed of a general set and refined set of protein−ligand complexes. The general set consists of 12 800 complexes and the refined set consists of 4852 complexes. Due to the observed redundancy of the proteins represented in the PDBbind database, the UniProt-KB[28] IDs of the proteins were used to identify redundant proteins and retain only a unique representative of the protein. The scPDB database consists of 17 594 complexes, which were compared to both PDBbind general and refined set complexes. After removing overlapping and redundant complexes and active sites with nonstandard amino acids, the PDBbind general set, refined set, and scPDB database were combined to obtain a total of 5981 active sites for training the GAT-VAE model. All preprocessing steps were done through in-house perl and python scripts.

Model. The GAT-VAE model is composed of an encoder and a decoder (Figure 1a). The adjacency matrix ($\mathbf{A}$) and node feature vector (X) of the graph are input to the encoder. After extensive hyperparameter tuning, the encoder consisted of five parallel attention heads with a hidden size of 128 dimensions each. This was followed by a single head GAT layer for aggregation of the output from the five parallel heads. The aggregated output node features are passed through two parallel single head GAT layers to obtain the mean and log variance vectors, which are subject to reparameterization to obtain the latent vector. A dropout rate of 0.2 was used to prevent overfitting of the model. Finally, the encoder returns a 256-dimensional latent vector (z) of the input active site graph. The decoder is a standard inner-product decoder which utilizes the latent vector to reconstruct the adjacency matrix of the input active site graph[29] (Figure S1d−f). The GAT-VAE model is trained to minimize a joint loss function composed of the binary cross entropy loss for adjacency matrix reconstruction and the Kullback−Leibler divergence (KLD) loss for enforcing the latent variables to follow the Gaussian distribution. Adam optimizer[30] was used to train the model with an initial learning rate of 0.001. The data set was split into minibatches of 256 graphs each. The model was trained for 100 epochs in a Tesla V100 GPU. All implementations were done in PyTorch.[31]

Two GAT-VAE models were trained with graph data sets constructed using different distance cut-offs for edge definition (4 and 5 Å). The model which exhibited the best ROC score in the adjacency matrix reconstruction task was used to condition the molecule generation process. The GAT-VAE model embeds the active site graphs into a latent representation so that they can be used later for conditional molecule generation.

Pretraining the SMILES-VAE Model to Learn the Grammar of Small Molecules. *Data.* The data set of drug-like small molecules in SMILES format was obtained from the ChEMBL database.[32] The SMILES data set was preprocessed by following the procedure from our previous study.[9] The RDKit library[33] was used for data set preprocessing.

Model. The data set of ∼1.6 million drug-like small molecules in SMILES format was used for pretraining the generative model. The deep neural network architecture of the SMILES-VAE model consists of an encoder and a decoder (Figure 1b). Both encoder and decoder consist of two layers of 1024 bidirectional gated recurrent units (GRU) as the internal memory, augmented with a stack acting as the dynamic external memory.[34] The stack had a width of 256 units and a depth of 100 units. An embedding layer and a dense layer with

https://doi.org/10.1021/acs.jcim.1c01319
J. Chem. Inf. Model. 2022, 62, 5100−5109

log softmax activation were used to pass the input to the encoder and retrieve the output from the decoder, respectively.

Training was performed using mini-batch gradient descent with AMSGrad optimizer.[35] The batch size and initial learning rate were set to 256 and 0.0005, respectively. A dropout rate of 0.2 was used to prevent overfitting of the model. Learning rate decay and gradient clipping were used to prevent vanishing and exploding gradients. The model was trained for 100 epochs on a Tesla V100 GPU, and the weights from the trained model were used for the downstream tasks in the pipeline. All implementations were done in PyTorch.[31]

Conditional Molecule Generator by Combining the Pretrained VAE Models. The pretrained GAT-VAE and SMILES-VAE models were combined (Figure 1c) to condition the molecule generation process to generate molecules specific to the target protein. To condition the SMILES-VAE model, the latent vector of the input graph (z_g) from the GAT-VAE encoder was concatenated with the latent vector corresponding to a primer string (z_s) from the SMILES-VAE encoder, to form the combined latent vector (z). The primer string usually corresponds to the SOS character (!), which can also be replaced by a scaffold or molecular group that needs to be present in the generated small molecule.[36] The conditional molecule generator was pretrained with the unique active site—small molecule pairs from the PDBbind data set[26] (general set and refined set). This short pretraining enabled the SMILES-VAE decoder to learn to decode the combined latent vector (z) with more chemical validity in comparison to the model without pretraining.

The pretraining of conditional molecule generator was done with AMSGrad optimizer[35] for 50 epochs, with an initial learning rate of 0.0005 and a batch size of 256. The cross-entropy loss for the reconstruction of the small molecule corresponding to the active site was used for training.

Pretraining the Drug-Target Affinity (DTA) Prediction Model. *Data.* The drug-target affinity (DTA) prediction model requires a training data set of active small molecules against various target proteins. This data set should include small molecules spanning both the high and low ends of the bioactivity spectrum, to improve the generalizability of the DTA model for novel small molecules.[37] All active site−small molecule pairs from the PDBbind general set and refined set with experimentally determined IC_{50}, K_i, and K_d values were collected amounting to a set of 9584 unique data points. All the data points were scaled to their corresponding molar concentrations and converted to log scale.[37]

Model. A drug-target affinity (DTA) prediction model was built to measure the affinity of the generated small molecules toward the target protein (Figure 1d). The DTA model used in this work is based on the extended connectivity interaction fingerprints (ECIF) developed in a previous study.[38] ECIF is used to represent a protein−ligand complex as a vector of 1540 integer-valued features, where each position corresponds to the count of a pairwise combination of protein−ligand atom types with preserved directionality. Therefore, the protein−ligand complexes from the general and refined set of PDBbind data set were used to train the DTA model with ECIF fingerprints and 170 RDKit chemical descriptors as inputs.[38] The DTA model is a gradient-boosted tree (GBT) built using the hyperparameters described in the ECIF study: 20 000 boosting stages, maximum depth of 8, a learning rate of 0.005, least-squares regression as the loss function, a fraction of samples to fit the individual learners of 0.7, and "sqrt" as the fraction of features to look at for the best split.[38] The Pearson correlation coefficient (r) and the root-mean-square error (RMSE) were used as the metrics to assess the model performance. The model was validated on the PDBbind core set and tested on the Astex diversity set.[39]

Design of Novel Small Molecules with Optimized Binding Affinity Using an RL Framework. The reinforcement learning framework combines the conditional molecule generator (agent) and the DTA model (critic) to design novel small molecules for any given target protein (Figure 1e). The generation and optimization cycle starts by providing the active site graph of the target protein as input to the conditional molecule generator. During a single iteration, 50 molecules are sampled using the conditional molecule generator for an input active site graph and passed to the DTA model (critic) for evaluation. The number of molecules to be sampled per iteration was chosen based on extensive hyperparameter tuning. The DTA model predicts the pIC_{50} value of each generated molecule with respect to the target active site. The protein−ligand complex required to compute the ECIF fingerprints for the generated small molecules was obtained through on-the-fly docking of molecules to the target active site using gnina.[40] This predicted pIC_{50} value is used to calculate the reward/penalty using a reward function 1.

$$r(x) = \exp\left(\frac{x}{3.0}\right) \tag{1}$$

Here, x refers to the predicted pIC_{50} value of the generated molecule. The reward/penalty from the reward function is used in a regularized loss function which prevents "catastrophic forgetting" of the features learnt by the model.[5] The generation and optimization cycle continues until the bioactivity distribution for the generated small molecules is well optimized. Termination of the RL training process is target protein-dependent, and multiple criteria are considered including, validity of the generated molecules, presence of duplicates, extent of bioactivity optimization, and rate of reproduction of molecules from the training data set (ChEMBL database).

Validation of the Generated Small Molecules after RL Training. *Data.* An *in silico* validation was performed to understand the quality of the generated molecules. The generated molecules were compared with small molecules specific to two target proteins—Janus kinase 2 (JAK2) and dopamine receptor D2 (DRD2). The data sets of all known inhibitors of JAK2 and DRD2 along with their experimentally determined pIC_{50} values, were collected from the ChEMBL database.[32] These data sets were preprocessed following the procedure from our previous study[9] after which, the JAK2 and DRD2 validation data sets contained 1103 and 4221 compounds, respectively. The JAK2 and DRD2 validation set ligands in combination with the JAK2 and DRD2 receptor were not part of any of the training sets.

Analysis. After the RL training, a set of 10 000 small molecules were generated with predicted bioactivity values for each of the target proteins. The quality of the generated small molecules was validated by measuring the similarity of the generated small molecules to known ligands of the target protein (validation data set, mentioned earlier), based on the Tanimoto coefficient.[41] The similarity of various physicochemical property distributions of generated small molecules and known ligands were also compared. In terms of the substructure similarity, two different analyses, (a) fragment

https://doi.org/10.1021/acs.jcim.1c01319
J. Chem. Inf. Model. 2022, 62, 5100−5109

Table 1. Benchmarking Results: Comparison between the Benchmark Metrics of the Baseline VAE Model from the GuacaMol Benchmark and the SMILES-VAE Model in This Study

model	validity	uniqueness	novelty	Fréchet ChemNet distance (FCD)	Kullback−Leibler divergence (KLD)
GuacaMol baseline VAE model[44]	0.870	0.999	0.974	0.863	0.982
SMILES-VAE model	0.932	0.999	0.969	0.847	0.981

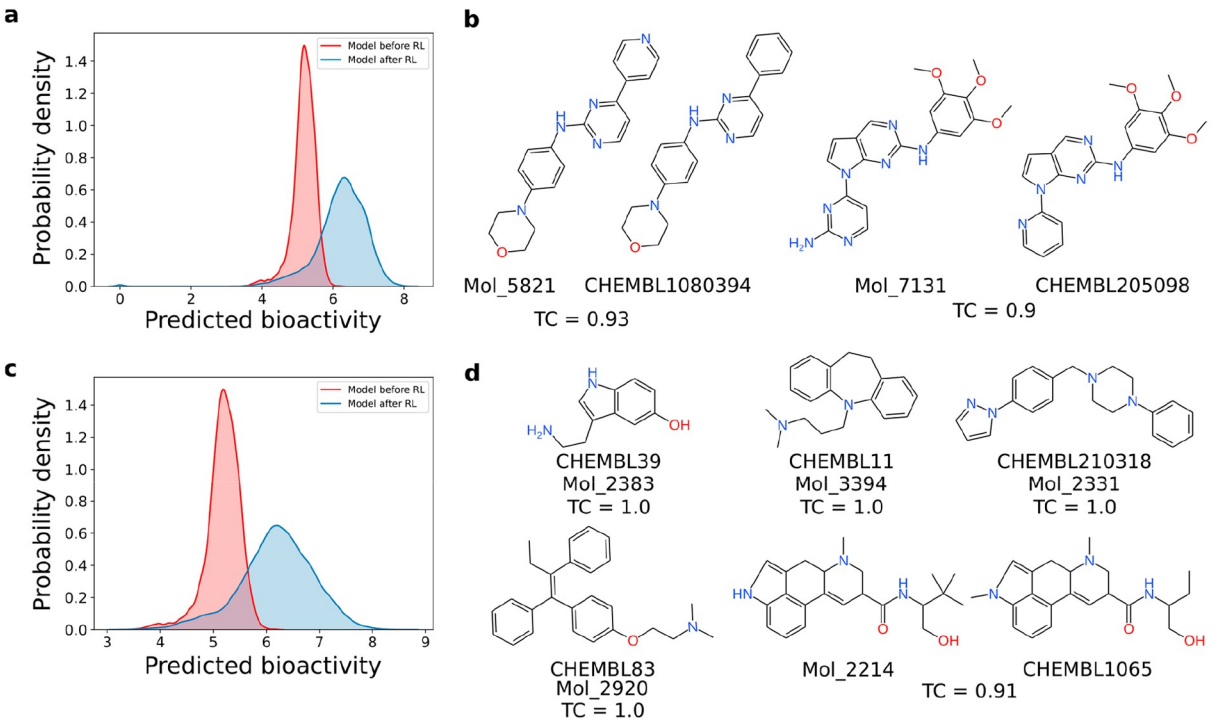

Figure 2. Predicted bioactivity distributions based on the DTA model for the generated small molecules specific to (a) JAK2 and (c) DRD2 before and after reinforcement learning, along with examples of generated small molecules with high similarity to existing inhibitors of (b) JAK2 and (d) DRD2. The CHEMBL identifiers or PubChem CIDs of the known inhibitors are also provided for each molecule.

distribution and (b) pharmacophore-based screening, were performed. The pharmacophore-based screening helped to explain the geometric arrangement of atoms or functional groups of the generated molecules, that are essential for target inhibition. While the Tanimoto coefficient enabled identification of generated molecules that are similar to the validation data set, the latter two substructure analysis methods helped to identify molecules with spatial features similar to the validation data set, albeit with diversity.

The PharmaGist program[42] was used for ligand-based pharmacophore analysis. To extract the ligand-based pharmacophores, the existing inhibitors of the target protein were clustered using Butina clustering[43] in RDKit with Tanimoto coefficient as the distance metric and 0.4 as the distance cutoff. Since the PharmaGist program can take only 32 molecules as input, clustering was used to narrow down the size of the validation data set. From the clustering results, clusters with at least 10 molecules were chosen and the representative molecules of such clusters were collected. A random set of 32 molecules from this list was used as input to the PharmaGist program. The top two composite ligand-based pharmacophores were chosen based on coverage of the active site and the ability to represent at least 95% of the molecules present in the validation data set. They were used to screen the database of generated small molecules specific to the target protein of interest.

RESULTS

Performance of the Pretrained Models. The SMILES-VAE model pretrained on the ChEMBL data set was evaluated using the GuacaMol distribution learning benchmark (v0.5.3).[44] The metrics of the benchmark include: validity, uniqueness, novelty, Kullback−Leibler divergence (KLD), and Fréchet ChemNet distance (FCD). The SMILES-VAE model is 93.22% accurate in decoding SMILES strings from their latent representations, with 99% uniqueness and 96% novelty among the sampled small molecules. In comparison to the baseline VAE model highlighted in the GuacaMol benchmark, the pretrained SMILES-VAE model in this study excelled in the validity metric (Table 1). The distributions of the various physicochemical properties of the generated small molecules in comparison to the ChEMBL data set has been provided in the Supporting Information (Figure S2).

As mentioned in the Materials and Methods, two different GAT-VAE models were trained on active site graph data sets created with two distance cut-offs for edge definition: (A) model 1 with 4 Å and (B) model 2 with 5 Å. The models were trained on the task of reconstructing the adjacency matrix from the latent embedding of the active site graph. The ROC scores for models 1 and 2 were 0.89 and 0.84, respectively. Based on the validation ROC scores, edge permutation tests, and cues from the literature on protein interaction networks,[24] model 1 was chosen for further analyses.

https://doi.org/10.1021/acs.jcim.1c01319
J. Chem. Inf. Model. 2022, 62, 5100−5109

Table 2. Results from the Pharmacophore-Based Screening of Generated Small Molecules for JAK2 and DRD2 Proteins[a]

protein	pharmacophore	hits[b] (%)	screened count[c]	not screened count	screened by the other pharmacophore	not screened by both pharmacophores
DRD2 validation set	pharmacophore 1	97.26	4162	44	39	5
	pharmacophore 2	97.95	4158	48	43	
DRD2 generated set	pharmacophore 1	84.63	8475	761	329	432
	pharmacophore 2	85.09	8399	837	405	
JAK2 validation set	pharmacophore 1	99.72	1103	0	0	0
	pharmacophore 2	100	1103	0	0	
JAK2 generated set	pharmacophore 1	87.45	8577	27	15	12
	pharmacophore 2	94.76	8588	16	4	

[a]The percentage of hits, number of molecules screened by either pharmacophores, and molecules which are not screened by both the pharmacophores are provided. [b]Percentage of molecules with at least half the maximum overlap score are considered as hits. [c]Any molecule with a positive overlap score is considered as a screened molecule.

The drug-target affinity prediction model was validated with the PDBbind core set and tested with the Astex diversity set.[39] The Pearson correlation coefficient (r) and root-mean-square error (RMSE) were used as the evaluation metrics for the model. The Pearson correlation coefficient (R_p) for PDBbind core set and Astex diversity set after 5-fold cross-validation was 0.851 (RMSE = 1.21) and 0.565 (RMSE = 1.52), respectively (Table S1). The regression plots for the predicted versus actual bioactivity values of the PDBbind core set and Astex diversity set are provided in Supporting Information (Figure S3). It is notable that the DTA model in this work performs better (in terms of R_p) than the existing DTA models for the Astex diversity set.[37,45,46]

Generating Novel Small Molecules against JAK2 and DRD2. The pretrained conditional VAE model was used as the agent in a reinforcement learning framework, along with the DTA prediction model as the critic, to generate novel small molecules specific to the target proteins. Two well-studied proteins—JAK2 (PDB ID: 3UGC), an intracellular protein belonging to the ubiquitous kinase family, and DRD2 (PDB ID: 6CM4), a G-protein coupled receptor (GPCR) present in the central nervous system, were chosen. The large number of available inhibitors for JAK2 and DRD2 provides an opportunity for *in silico* validation of the proposed method.

For each target protein, the conditional molecule generator was trained individually using the corresponding binding site graph until a sufficient shift in the distribution of bioactivity values (predicted by DTA model) was observed. The final bioactivity distributions obtained after the training process are shown above (Figure 2, parts a and c). After the reinforcement learning training process, the resultant target-specific conditional molecule generator model was used to sample 10 000 small molecules. Molecules that were chemically invalid were removed, and the rest of the molecules were canonicalized before further analysis. In both the cases, the model after reinforcement learning could generate an average of 90% valid molecules indicating that the model has overcome catastrophic forgetting effectively. The set of physicochemical property distributions after reinforcement learning for each target protein studied, is provided in the Supporting Information (Figures S4 and S5).

Analysis of the Generated Small Molecules. An *in silico* validation of the method was performed by comparing existing inhibitors of the target proteins with the generated molecules. The similarity of the generated molecules was checked in terms of Tanimoto coefficient and pharmacophoric distributions.

A. Similarity of Generated Molecules Based on Tanimoto Coefficient. First the similarity of the generated small molecules to a target-specific data set of molecules was computed using the Tanimoto coefficient (TC) with ECFP4 fingerprints[47] as input representations. A TC cutoff of 0.75 was used to identify the subset of generated molecules which have high similarity to existing molecules for a target protein. On the basis of the comparison, it was identified that 30 and 80 generated small molecules met the TC cutoff requirement for JAK2 and DRD2 proteins, respectively (Figure 2, parts b and d). Furthermore, five generated small molecules were also found to be identical with the existing DRD2 inhibitors (TC = 1.0), showcasing the ability of the conditional generative model to reproduce existing inhibitors for a target protein.

One of the limitations of TC-based scoring of ECFP4 fingerprints is that it does not consider the feature similarities among functional groups present in the two molecules.[48] This leads to identification of only a subset of generated molecules whose structure is extremely similar to the existing inhibitors, but misses the other diverse molecules, which can still possess the required functional groups, or the pharmacophore features necessary for biological response.

B. Similarity of the Generated Molecules Based on Ligand-Based Pharmacophores. The ligand-based pharmacophores extracted using the PharmaGist program[42] were used to screen the generated small molecules and identify molecules with high feature overlap score. Such molecules can be considered as efficient inhibitors despite their lower ECFP4-based Tanimoto similarity compared to existing inhibitors.

A small molecule was considered as a hit, if the feature overlap score of the molecule with the target pharmacophore was at least half of the maximum feature overlap score. The hits among the generated small molecules were filtered for both JAK2 and DRD2 proteins. The results of the pharmacophore-based screening are summarized in Table 2. On the basis of the results, it is observed that 87% of the JAK2-specific generated molecules and 84% of the DRD2-specific generated molecules could be covered by the target-specific ligand-based pharmacophores of the respective proteins. The two selected composite ligand-based pharmacophores of the DRD2 protein are shown in Supporting Information (Figure S6, parts c and d).

Similar to DRD2, two pharmacophores were identified based on the coverage of the active site of JAK2 (Figure S6, parts a and b). A few examples of JAK2-specific generated molecules with high pharmacophore-level similarity, but low ECFP4-based Tanimoto similarity (less than 0.60) to existing

https://doi.org/10.1021/acs.jcim.1c01319
J. Chem. Inf. Model. 2022, 62, 5100−5109

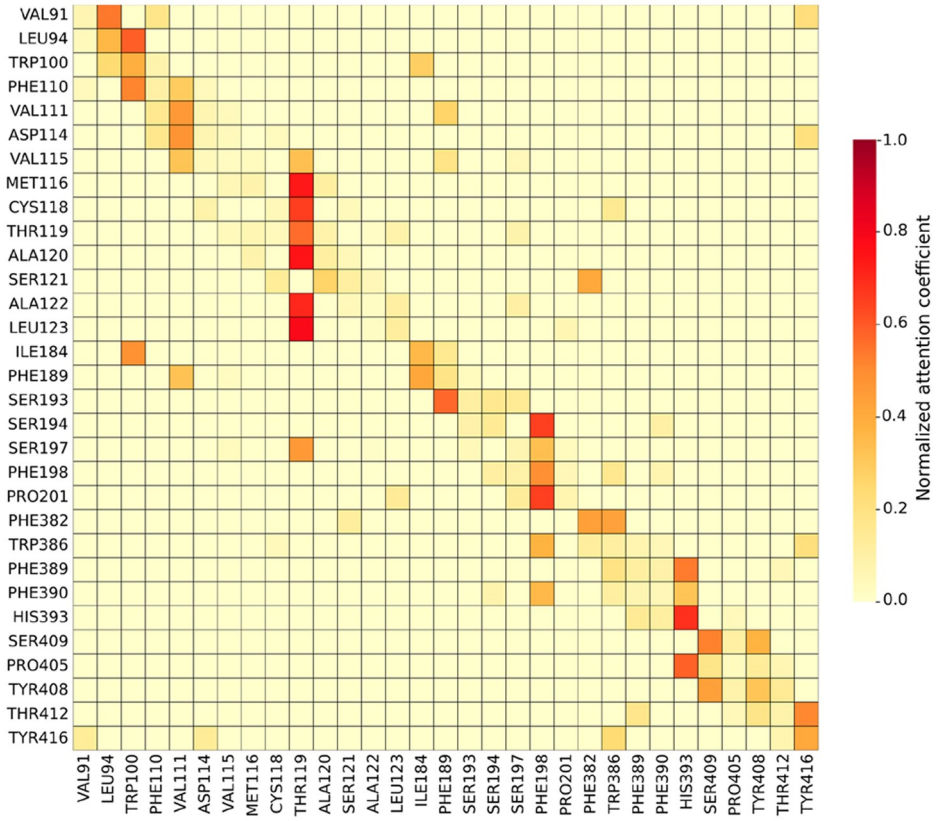

Figure 3. Heatmap of attention coefficients for the active site residues of dopamine receptor D2 (DRD2) protein (PDB ID: 6CM4). The residues are ordered according to their position in the sequence of the protein. Darker boxes indicate higher attention coefficients and more importance to the interaction between the pair of residues.

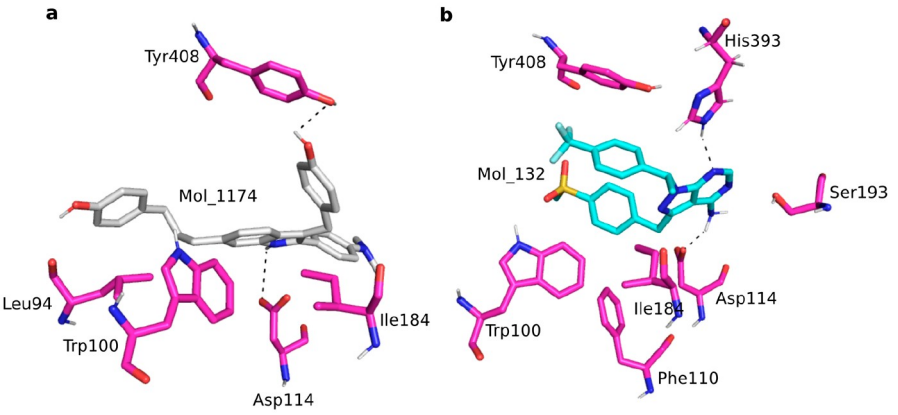

Figure 4. Interactions between key active site residues identified from attention coefficients and selected DRD2-specific generated small molecules: (a) Mol_1174 (white sticks) and (b) Mol_132 (cyan sticks). The residues forming hydrogen bond are shown as dotted lines.

inhibitors, are shown in Figure S7. It is clear from the pharmacophore-based screening results that the generated small molecules capture the key pharmacophore features of the target active site. To further confirm the pharmacophore-level similarity of the generated small molecules to the existing inhibitors, two pharmacophore fingerprints (ErGFP and PharmacoPFP) were calculated following a recent study.[49] The pharmacophore fingerprints of generated small molecules and existing inhibitors were compared using cosine similarity. The distribution of the cosine similarity values from all pairwise comparisons (Figure S8) shows that above 90% of the generated small molecules have high pharmacophore-level similarity (cosine similarity above 0.8) to existing inhibitors.

Important Active Site Residues from the GAT-VAE Model. The attention coefficients from the GAT-VAE model were analyzed for each residue (node) and its neighborhood in the active site graph. In essence, the attention coefficients define an interaction probability distribution over each node and its neighbors in the graph. By analyzing the attention coefficients for each node, the residue pairs which are frequently given more attention by the model can be identified, and the biological significance behind the latent representation learned by the GAT-VAE model can be elucidated. By

https://doi.org/10.1021/acs.jcim.1c01319
J. Chem. Inf. Model. 2022, 62, 5100−5109

considering the attention coefficients of a node's neighborhood as probabilities, the information content of the coefficients can be calculated using Shannon's entropy.[50] Skewness in the entropy distribution compared to the uniform distribution indicates that, the model has learned to give importance to a subset of node neighbors, rather than providing equal weight for all the neighbors of a given node (Figure S9).

The key residues and interactions at the DRD2 binding site identified from the attention coefficient heatmap are shown in Figure 3. Residue pairs with attention coefficients above 0.5 were considered important. For the binding site of the DRD2 protein (PDB ID: 6CM4), only 17 of the 149 interactions had attention coefficient (α_{ij}) above 0.50 from the GAT-VAE model. The eight active site residues (Leu94, Trp100, Asp114, Thr119, Ile184, Phe198, His393, and Tyr416) are involved with attention coefficients above 0.5. These eight active site residues are known to interact with various highly selective DRD2 inhibitors reported in the literature.[51−53] These residues were also found to interact with generated molecules. The interactions between two representative generated molecules with these key active site residues are shown in Figure 4. The active site of DRD2 is partially hydrophobic (Leu94, Trp100, Ile184, Phe110). These residues form hydrophobic interactions with the generated molecules. However, on the other side, it is lined with polar and charged residues (Asp114, Thr119, Ser193, His393, and Tyr408), which form hydrogen bond interactions with the generated molecules. Additionally, Tyr408 can also form stacking interactions with the generated molecules.

Three stabilizing interactions among DRD2 active site residues—His393 and Tyr408 (α_{ij} = 0.6), Ile184 and Trp100 (α_{ij} = 0.5), and Trp100 and Leu94 (α_{ij} = 0.6) are also reported in the previous literature.[51] It is interesting to note that, mutation studies have proven the importance of interactions between Leu94, Trp100, and Ile184 in stabilizing the protein−ligand complex, and dissociation of the ligand from the binding site.[51] Also, an interhelical hydrogen bond between His393 and Tyr408 has been shown to stabilize the outward movement of the transmembrane helix VI in DRD2, which controls the switch between active and inactive states of the protein.[51] The presence of a secondary amine group in the vicinity of the active site residue Asp114, helps in hydrogen bond formation (Figure 4). According to the previous literature, the Asp114 interaction is responsible to anchor the small molecules in the active site cavity.[52] Overall, the residue pairs with higher attention coefficients were found to provide stability to the generated molecules and their role is also known from previous literature. Deep learning models are often criticized as black boxes, but the method proposed in this work could explain the importance of active site residues. Possibly, these residues play a role in molecule generation, which can be explained from the complementarity of interactions with the generated molecules in case of DRD2 protein (Figure 4).

The key binding site residues of JAK2 active site, those governing the interactions with generated small molecules and identified from the attention coefficient heatmap (see Figure S10) is discussed in detail in the Supporting Information (Sections 1 and 2). The selectivity of generated small molecules toward JAK2 was also checked and discussed in the Supporting Information (Section 3).

These observations show that the GAT-VAE model can distinguish key binding site residues and interactions from the rest and incorporate that information in the latent representation of the active site graph by learning sharper attention coefficients. This also shows the usefulness of attention-based methods in enabling a better understanding of the features learned by the deep neural network model from a biological standpoint.

CONCLUSIONS

In this study, a new structure-based method for designing novel small molecules was developed using deep learning. The method utilizes a combination of a graph attention network and a stack-augmented recurrent neural network to form a conditional generative model. It can generate small molecules specific to a target active site under the guidance of a drug-target affinity prediction model. The graph attention model was able to distinguish the key active site residues and inter-residue interactions through the attention coefficients, which was visualized using entropy histograms and the attention coefficient heatmap. The use of active site information in the form of an active site graph and the ECIF fingerprint helps to generate molecules specific to a target protein of interest. The conditional generative model was validated on two different target proteins and was found to generate small molecules with high similarity compared to the existing inhibitors. The generated small molecules were also found to preserve the key pharmacophoric features required to efficiently bind to the active site of the target protein.

The method developed in this study can be utilized for any target protein whose three-dimensional structure is known from either experimental or molecular modeling methods. Also, in the current work, the active site of the target protein was assumed to be composed of only the 20 standard amino acid residues. In future, we would like to include the contribution of cofactors bound to the active site (metal ions, heme, and others) and common nonstandard amino acids during the molecule generation process.

ASSOCIATED CONTENT

Supporting Information

The Supporting Information is available free of charge at https://pubs.acs.org/doi/10.1021/acs.jcim.1c01319.

Details of the results obtained for molecules designed against Janus kinase 2 protein, construction of the active site graph, various physicochemical property distributions of the generative model, composite pharmacophore, analysis using two different pharmacophore fingerprints, and 5-fold cross validation of drug target affinity prediction model (PDF)

Data set of generated small molecules along with their predicted bioactivity values (XLSX)

AUTHOR INFORMATION

Corresponding Author

Arijit Roy − *TCS Research (Life Sciences Division), Tata Consultancy Services Limited, Hyderabad 500081, India;* orcid.org/0000-0002-1961-2483; Email: roy.arijit3@tcs.com

Authors

Sowmya Ramaswamy Krishnan − *TCS Research (Life Sciences Division), Tata Consultancy Services Limited,*

https://doi.org/10.1021/acs.jcim.1c01319
J. Chem. Inf. Model. 2022, 62, 5100−5109

Hyderabad 500081, India; orcid.org/0000-0001-5404-3266

Navneet Bung − *TCS Research (Life Sciences Division), Tata Consultancy Services Limited, Hyderabad 500081, India;* orcid.org/0000-0002-6376-277X

Sarveswara Rao Vangala − *TCS Research (Life Sciences Division), Tata Consultancy Services Limited, Hyderabad 500081, India*

Rajgopal Srinivasan − *TCS Research (Life Sciences Division), Tata Consultancy Services Limited, Hyderabad 500081, India*

Gopalakrishnan Bulusu − *TCS Research (Life Sciences Division), Tata Consultancy Services Limited, Hyderabad 500081, India;* orcid.org/0000-0002-4958-7573

Complete contact information is available at: https://pubs.acs.org/10.1021/acs.jcim.1c01319

Author Contributions

#S.R.K. and N.B. had equal contributions.

Notes

The authors declare the following competing financial interest(s): All the authors were employed by Tata Consultancy Services Limited.

Data and Software Availability. All input data are publicly available and a detailed description for the same is mentioned in the Materials and Methods. The code used to generate results shown in this study is available from the corresponding author upon request for academic use only.

REFERENCES

(1) Öztürk, H.; Özgür, A.; Schwaller, P.; Laino, T.; Ozkirimli, E. Exploring chemical space using natural language processing methodologies for drug discovery. *Drug Discovery Today* **2020**, *25*, 689−705.

(2) Xiong, J.; Xiong, Z.; Chen, K.; Jiang, H.; Zheng, M. Graph neural networks for automated de novo drug design. *Drug Discovery Today* **2021**, *26*, 1382−1393.

(3) Skalic, M.; Sabbadin, D.; Sattarov, B.; Sciabola, S.; De Fabritiis, G. From Target to Drug: Generative Modeling for the Multimodal Structure-Based Ligand Design. *Mol. Pharmaceutics* **2019**, *16*, 4282−4291.

(4) Kirkpatrick, P.; Ellis, C. Chemical Space. *Nature* **2004**, *432*, 823.

(5) Olivecrona, M.; Blaschke, T.; Engkvist, O.; Chen, H. Molecular *De-Novo* Design Through Deep Reinforcement Learning. *J. Cheminf.* **2017**, *9*, 48.

(6) Popova, M.; Isayev, O.; Tropsha, A. Deep Reinforcement Learning for De Novo Drug Design. *Sci. Adv.* **2018**, *4*, eaap7885.

(7) Sattarov, B.; Baskin, I. I.; Horvath, D.; Marcou, G.; Bjerrum, E. J.; Varnek, A. De Novo Molecular Design by Combining Deep Autoencoder Recurrent Neural Networks with Generative Topographic Mapping. *J. Chem. Inf. Model.* **2019**, *59*, 1182−1196.

(8) Born, J.; Manica, M.; Cadow, J.; Markert, G.; Mill, N. A.; Filipavicius, M.; Janakarajan, N.; Cardinale, A.; Laino, T.; Rodríguez Martínez, M. R. Data-driven molecular design for discovery and synthesis of novel ligands: a case study on SARS-CoV-2. *Mach. Learn.: Sci. Technol.* **2021**, *2*, 025024.

(9) Krishnan, S. R.; Bung, N.; Bulusu, G.; Roy, A. Accelerating De Novo Drug Design against Novel Proteins Using Deep Learning. *J. Chem. Inf. Model.* **2021**, *61*, 621−630.

(10) Bung, N.; Krishnan, S. R.; Bulusu, G.; Roy, A. De novo design of new chemical entities for SARS-CoV-2 using artificial intelligence. *Future Med. Chem.* **2021**, *13*, 575−585.

(11) Gómez-Bombarelli, R.; Wei, J. N.; Duvenaud, D.; Hernández-Lobato, J. M.; Sánchez-Lengeling, B.; Sheberla, D.; Aguilera-Iparraguirre, J.; Hirzel, T. D.; Adams, R. P.; Aspuru-Guzik, A. Automatic Chemical Design Using a Data-Driven Continuous Representation of Molecules. *ACS Cent. Sci.* **2018**, *4*, 268−276.

(12) Gao, K.; Nguyen, D. D.; Tu, M.; Wei, G. Generative Network Complex for the Automated Generation of Drug-like Molecules. *J. Chem. Inf. Model.* **2020**, *60*, 5682−5698.

(13) Winter, R.; Montanari, F.; Steffen, A.; Briem, H.; Noé, F.; Clevert, D. Efficient multi-objective molecular optimization in a continuous latent space. *Chem. Sci.* **2019**, *10*, 8016−8024.

(14) Zhavoronkov, A.; Ivanenkov, Y. A.; Aliper, A.; Veselov, M. S.; Aladinskiy, V. A.; Aladinskaya, A. V.; Terentiev, V. A.; Polykovskiy, D. A.; Kuznetsov, M. D.; Asadulaev, A.; Volkov, Y.; Zholus, A.; Shayakhmetov, R. R.; Zhebrak, A.; Minaeva, L. I.; Zagribelnyy, B. A.; Lee, L. H.; Soll, R.; Madge, D.; Xing, L.; Guo, T.; Aspuru-Guzik, A. Deep learning enables rapid identification of potent DDR1 kinase inhibitors. *Nat. Biotechnol.* **2019**, *37*, 1038−1040.

(15) Stokes, J. M.; Yang, K.; Swanson, K.; Jin, W.; Cubillos-Ruiz, A.; Donghia, N. M.; MacNair, C. R.; French, S.; Carfrae, L. A.; Bloom-Ackermann, Z.; Tran, V. M.; Chiappino-Pepe, A.; Badran, A. H.; Andrews, I. W.; Chory, E. J.; Church, G. M.; Brown, E. D.; Jaakkola, T. S.; Barzilay, R.; Collins, J. J. A Deep Learning Approach to Antibiotic Discovery. *Cell* **2020**, *180*, 688−702.

(16) Batool, M.; Ahmad, B.; Choi, S. A Structure-Based Drug Discovery Paradigm. *Int. J. Mol. Sci.* **2019**, *20*, 2783.

(17) Aumentado-Armstrong, T. Latent Molecular Optimization for Targeted Therapeutic Design *ArXiv* 2018; https://arxiv.org/abs/1809.02032.

(18) Grechishnikova, D. Transformer neural network for protein-specific de novo drug generation as a machine translation problem. *Sci. Rep.* **2021**, *11*, 321.

(19) Veličković, P.; Cucurull, G.; Casanova, A.; Romero, A.; Liò, P.; Bengio, Y. Graph Attention Networks. In *Proceedings of the International Conference on Learning Representations, Vancouver, Canada, April 3−May 3, 2018*, 2018.

(20) Weininger, D.; Weininger, A.; Weininger, J. L. SMILES. 2. Algorithm for Generation of Unique SMILES Notation. *J. Chem. Inf. Comput. Sci.* **1989**, *29*, 97−101.

(21) Chung, J.; Gulcehre, C.; Cho, K.; Bengio, Y. Empirical Evaluation of Gated Recurrent Neural Networks on Sequence Modeling. In *NIPS 2014 Workshop on Deep Learning, Montréal, Canada, December 8−13, 2014*; 2014.

(22) Zamora-Resendiz, R.; Crivelli, S. Structural Learning of Proteins Using Graph Convolutional Neural Networks *bioRxiv* 2019; https://www.biorxiv.org/content/10.1101/610444v1.

(23) Torng, W.; Altman, R. B. Graph Convolutional Neural Networks for Predicting Drug-Target Interactions. *J. Chem. Inf. Model.* **2019**, *59*, 4131−4149.

(24) Chakrabarty, B.; Parekh, N. NAPS: Network Analysis of Protein Structures. *Nucleic Acids Res.* **2016**, *44*, W375−82.

(25) Shen, J.; Zhang, J.; Luo, X.; Zhu, W.; Yu, K.; Chen, K.; Li, Y.; Jiang, H. Predicting protein−protein interactions based only on sequences information. *Proc. Natl. Acad. Sci. U. S. A.* **2007**, *104*, 4337−41.

(26) Liu, Z.; Li, Y.; Han, L.; Li, J.; Liu, J.; Zhao, Z.; Nie, W.; Liu, Y.; Wang, R. PDB-wide collection of binding data: current status of the PDBbind database. *Bioinformatics* **2015**, *31*, 405−412.

(27) Desaphy, J.; Bret, G.; Rognan, D.; Kellenberger, E. sc-PDB: a 3D-database of ligandable binding sites - 10 years on. *Nucleic Acids Res.* **2015**, *43*, D399−D404.

(28) The UniProt Consortium. UniProt: the universal protein knowledgebase in 2021. *Nucleic Acids Res.* **2021**, *49*, D480−D489.

(29) Kipf, T. N.; Welling, M. Variational Graph Auto-Encoders *arXiv* 2016; https://arxiv.org/abs/1611.07308.

(30) Kingma, D. P.; Ba, J. Adam: A Method for Stochastic Optimization. In *Proceedings of International Conference on Learning Representations, San Diego, CA, May 7−9, 2015*; 2015.

(31) Paszke, A.; Gross, S.; Massa, F.; Lerer, A.; Bradbury, J.; Chanan, G.; Killeen, T.; Lin, Z.; Gimelshein, N.; Antiga, L.; Desmaison, A.; Köpf, A.; Yang, E.; DeVito, Z.; Raison, M.; Tejani, A.; Chilamkurthy, S.; Steiner, B.; Fang, L.; Bai, J.; Chintala, S. PyTorch: An Imperative

Style, High-Performance Deep Learning Library *arXiv* 2019; https://arxiv.org/abs/1912.01703.
(32) ChEMBL Database, version 27; DOI: 10.6019/CHEMBL.database.27 (accessed March 2021).
(33) Landrum, G. *RDKit: Open-Source Cheminformatics Software*; http://www.rdkit.org (accessed March 2021).
(34) Joulin, A.; Mikolov, T. Inferring Algorithmic Patterns with Stack-Augmented Recurrent Nets *Proceedings of the International Conference on Neural Information Processing Systems*, Montréal, Canada, December 7−12, *1*, 190−198, **2015**.
(35) Tran, P. T.; Phong, L. T. On the Convergence Proof of AMSGrad and a New Version. *IEEE Access* **2019**, *7*, 61706−61716.
(36) Born, J.; Manica, M.; Oskooei, A.; Cadow, J.; Markert, G.; Rodríguez Martínez, M. Paccmann^{RL}: Designing Anticancer Drugs from Transcriptomic Data via Reinforcement Learning. *IScience.* **2021**, *24*, 102269.
(37) Hassan-Harrirou, H.; Zhang, C.; Lemmin, T. RosENet: Improving Binding Affinity Prediction by Leveraging Molecular Mechanics Energies with an Ensemble of 3D Convolutional Neural Networks. *J. Chem. Inf. Model.* **2020**, *60*, 2791−2802.
(38) Sánchez-Cruz, N.; Medina-Franco, J. L.; Mestres, J.; Barril, X. Extended Connectivity Interaction Features: Improving Binding Affinity Prediction Through Chemical Description. *Bioinformatics* **2021**, *37*, 1376.
(39) Hartshorn, M. J.; Verdonk, M. L.; Chessari, G.; Brewerton, S. C.; Mooij, W. T. M.; Mortenson, P. N.; Murray, C. W. Diverse, High-Quality Test Set for the Validation of Protein−Ligand Docking Performance. *J. Med. Chem.* **2007**, *50*, 726−741.
(40) McNutt, A. T.; Francoeur, P.; Aggarwal, R.; Masuda, T.; Meli, R.; Ragoza, M.; Sunseri, J.; Koes, D. R. GNINA 1.0: molecular docking with deep learning. *J. Cheminf.* **2021**, *13*, 43.
(41) Lipkus, A. H. A Proof of the Triangle Inequality for the Tanimoto Distance. *J. Math. Chem.* **1999**, *26*, 263−265.
(42) Schneidman-Duhovny, D.; Dror, O.; Inbar, Y.; Nussinov, R.; Wolfson, H. J. PharmaGist: a webserver for ligand-based pharmacophore detection. *Nucleic Acids Res.* **2008**, *36*, W223−8.
(43) Butina, D. Unsupervised Data Base Clustering Based on Daylight's Fingerprint and Tanimoto Similarity: A Fast and Automated Way To Cluster Small and Large Data Sets. *J. Chem. Inf. Comput. Sci.* **1999**, *39*, 747−750.
(44) Brown, N.; Fiscato, M.; Segler, M. H. S.; Vaucher, A. C. GuacaMol: Benchmarking Models for de Novo Molecular Design. *J. Chem. Inf. Model.* **2019**, *59*, 1096−1108.
(45) Stepniewska-Dziubinska, M. M.; Zielenkiewicz, P.; Siedlecki, P. Development and Evaluation of a Deep Learning Model for Protein−Ligand Binding Affinity Prediction. *Bioinformatics* **2018**, *34*, 3666−3674.
(46) Zheng, L.; Fan, J.; Mu, Y. OnionNet: A Multiple-Layer Intermolecular-Contact-Based Convolutional Neural Network for Protein−Ligand Binding Affinity Prediction. *ACS Omega.* **2019**, *4*, 15956−15965.
(47) Rogers, D.; Hahn, M. Extended-connectivity fingerprints. *J. Chem. Inf. Model.* **2010**, *50*, 742−54.
(48) Stiefl, N.; Watson, I. A.; Baumann, K.; Zaliani, A. ErG: 2D Pharmacophore Descriptions for Scaffold Hopping. *J. Chem. Inf. Model.* **2006**, *46*, 208−220.
(49) Shen, W. X.; Zeng, X.; Zhu, F.; Wang, Y. L.; Qin, C.; Tan, Y.; Jiang, Y. Y.; Chen, Y. Z. Out-of-the-box deep learning prediction of pharmaceutical properties by broadly learned knowledge-based molecular representations. *Nat. Mach. Intell.* **2021**, *3*, 334−343.
(50) Shannon, C. E. A Mathematical Theory of Communication. *Bell Syst. Tech. J.* **1948**, *27*, 623−656.
(51) Wang, S.; Che, T.; Levit, A.; Shoichet, B. K.; Wacker, D.; Roth, B. L. Structure of the D2 dopamine receptor bound to the atypical antipsychotic drug risperidone. *Nature* **2018**, *555*, 269−273.
(52) Fan, L.; Tan, L.; Chen, Z.; Qi, J.; Nie, F.; Luo, Z.; Cheng, J.; Wang, S. Haloperidol bound D_2 dopamine receptor structure inspired the discovery of subtype selective ligands. *Nat. Commun.* **2020**, *11*, 1074.
(53) Im, D.; Inoue, A.; Fujiwara, T.; Nakane, T.; Yamanaka, Y.; Uemura, T.; Mori, C.; Shiimura, Y.; Kimura, K. T.; Asada, H.; Nomura, N.; Tanaka, T.; Yamashita, A.; Nango, E.; Tono, K.; Kadji, F. M. N.; Aoki, J.; Iwata, S.; Shimamura, T. Structure of the dopamine D_2 receptor in complex with the antipsychotic drug spiperone. *Nat. Commun.* **2020**, *11*, 6442.